

M.A. Gruntman, Position-sensitive detectors based on microchannel plates (review), *Instruments and Experimental Techniques*, v.27, n.1, pt.1, p.1-19, 1984.

ISSN 0020-4412

Vol. 27, No. 1, Part 1, January-February, 1984

July, 1984

ИНЕТАК 27(1) 1-132 (1984)

INSTRUMENTS AND EXPERIMENTAL TECHNIQUES

ПРИБОРЫ И ТЕХНИКА ЭКСПЕРИМЕНТА
(PRIBORY I TEKHNIKA EKSPERIMENTA)

TRANSLATED FROM RUSSIAN

$\left(\frac{c}{b}\right)$ CONSULTANTS BUREAU, NEW YORK

Coordinate-sensitive detectors based on microchannel plates enable one to determine the coordinates of each recorded particle in digital form and are used in various types of physics experiment. The diameter of the sensitive surface may attain 10 cm, while the spatial resolution can be 10 μm . The survey presents a classification of these detectors in terms of the methods of determining the coordinates, and various types of these detectors are described along with their design features and electronic circuits, while the advantages and disadvantages of the different systems are discussed, along with the main areas of application.

1. INTRODUCTION

Many physics experiments are based on recording particle fluxes: ions, electrons, neutral atoms and molecules, or photons. One can use detectors based on secondary electron emission (secondary electron multipliers SEM) in order to convert from measuring integral characteristics to counting the individual particles, which greatly improves the sensitivity and accuracy. However, in some experiments this is insufficient and one needs position-sensitive detectors PSD to determine the coordinates of the arrival at the detector for each particle. There are various types of PSD [1, 2], and among these a special place is taken by detectors employing one of the forms of SEM: microchannel plates MCP. The threshold energies of particles recorded by such detectors are low. This means that the limit to the use of PSD based on MCP can be displaced to low energies (these are subsequently called CSD: coordinate-sensitive detectors), whereas PSD of other types are restricted almost entirely to nuclear physics.

CSD provide fairly high recording efficiency and coordinate digitization, so they can be used with computers to accumulate, process, and output the data, and it is also possible to record extremely weak spatially distributed fluxes. This is important for example in astronomy when strong probe fluxes may influence the object. Image digitization means that CSD can be used efficiently in space research and also in laboratories where the experiment strategy is dependent on the character of the results. Another line of CSD use is in examining particle flux characteristics. For this purpose, the CSD is used in combination with a dispersing element, which transforms the particle distribution with respect to some relevant parameter (mass, charge, energy, or momentum, or wavelength for photons) to give a spatial distribution. Up until recently, spatial distributions have been recorded by scanning or by the simultaneous use of several independent detectors. CSD not only substantially improve the speed and accuracy in such measurements but also enable one to perform experiments where traditional methods such as scanning would require unacceptably long times or would be quite impossible. CSD also enable one to perform multiparameter analysis, i.e., to determine not only the spatial distribution but also the time one. The CSD discussed below enable one to determine the time of arrival with an accuracy better than 1 nsec.

CSD based on MCP were devised about 15 years ago and since then have developed considerably. Certain CSD characteristics have been considered with various degrees of completeness in papers of survey type [1-6]. Here we give a classification of CSD in terms of the coordinate determination method, and we describe various types of CSD with features of their design and of the electronic circuits, and we discuss the advantages and disadvantages of these, together with the major CSD applications.

Space Research Institute, Academy of Sciences of the USSR, Moscow. Translated from *Pribery 1 Tekhnika Éksperimenta*, No. 1, pp. 14-29, January-February, 1984. Original article submitted January 25, 1983.

2. CSD DESIGN PRINCIPLE

Figure 1 shows the essential scheme for a CSD. The image to be recorded is produced by a particle flux at the surface of the converter 1. The image-forming method is determined by the form of the particles and by the particular application. Examples are provided by systems of optical or electrostatic lenses. The flux may vary from a few particles a second (in that case the image accumulation may require many hours) up to about 10^5 sec^{-1} . In the converter, the particles are converted to electrons; correspondingly, the particle flux is converted to an electron flux, which forms an image at the input surface of the first MCP. An example of a converter is a photocathode, which converts photons to electrons. The question of image transfer by electrons has been considered in detail in the literature [7] and is not one of the topics considered here. Often one can operate without a converter if the image is formed by a particle flux directly at the input surface of the first MCP. In that case, the particles should be recorded well by the MCP. This requires that the collision of a particle with the MCP should have a high probability of producing one or more electrons or else that the particle itself should be an electron of appropriate energy. For example, SEM record ultraviolet photons [8, 9] and x-ray ones [10, 11], as well as ions and neutral particles with energies exceeding a few hundred electron volts [12] as well as electrons [13]. The MCP block 2 (Fig. 1) consists of two MCP in series (one can also use three MCP [14]) with straight channels or else one MCP with curved ones [15], and this converts an input particle with a certain probability called the recording efficiency to give an electron avalanche of 10^4 - 10^6 electrons. (The use of dynode-type SEM for this purpose in CSD is only of historical interest [16, 17].) The electron avalanche emerging from the second MCP falls on the collector 3 (system of anodes), which enables one to determine the avalanche coordinates. This operation can be performed in two ways. In the first, one tends to reduce the transverse dimension of the avalanche at the collector, which is attained by applying appropriate potentials to the MCP and reducing the distance between the MCP even to the point of contact, as well as by reducing the distance between the second MCP and the collector to a few tens of microns. The position of the avalanche in that case can be determined with an accuracy no higher than that controlled by the size of the avalanche at the collector; the spatial resolution may be 50 μm . In the other method, one determines the position of the center of gravity of the avalanche; this usually requires that the characteristic transverse dimension of the avalanche at the collector is about 1 cm. This is attained by increasing the distance between the MCP and that between the second MCP and the collector. The center of gravity can be determined with an error of 20 μm .

To perform particle timing with an accuracy better than 1 nsec, one can use the signal recorded from the output of the second MCP. This signal is a positive-going pulse related to the escape of the electron avalanche from the MCP and can be derived without reference to the collector signals. To derive a timing signal independent of the coordinates, it is necessary to improve the conductivity of the MCP output surface, e.g., by gold coating [18]. Some actual and possible applications of the signal from the last MCP have been considered previously [19-23].

The electronic unit EU performing the recording and processing for the collector signals determines the center of gravity, which has a one-to-one relationship to the coordinates of the particle arriving at the input surface of the MCP unit. Then EU stores the coordinates and performs preliminary processing of the accumulated information, which may attain a very large volume in the construction of two-dimensional images, and it can modify the processing in accordance with the character of the collected information and can output various control commands and also output the information in a form convenient to the user. For this purpose, the EU includes a computer with control devices as well as accumulation and I/O ones. Also, the converter, MCP, and collector system operate under high vacuum ($\leq 10^{-6}$ torr), while the EU should have a high noise immunity, since CSD are frequently used under conditions where there are high levels of noise and interference (for example, on space vehicles).

3. MICROCHANNEL PLATES

There is an extensive literature [5, 7, 12, 15, 24-31] on the design, manufacturing technology, and characteristics of MCP for recording particles. Here we consider the most important aspects.

Two MCP placed in series and having straight channels may have diameters up to 10 cm and provide a gain K of about 10^7 (i.e., the electron avalanche at the output from the second MCP in recording a particle consists of about 10^7 electrons). If the two MCP are placed in

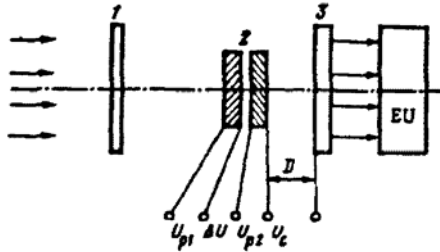


Fig. 1. Essential scheme for a CSD: 1) converter; 2) MCP unit; 3) collector; EU electronic unit.

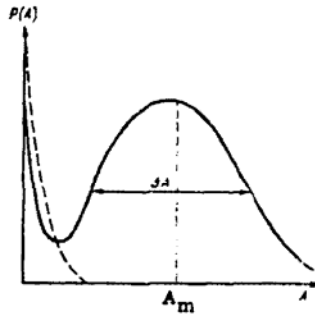


Fig. 2. Pulse-height distribution $P(A)$ characteristic of an MCP unit. The solid line is for particle recording, while the broken line is the inherent noise in the MCP unit; A_m is the most probable pulse height, while ΔA is the total width at half height.

such a way that the angle between the channels is 10° or more (the chevron configuration), one can substantially suppress ionic feedback, which is responsible for deterioration in the characteristics of the MCP unit. Similar characteristics can be attained by using a single MCP with curved channels, which simplifies the CSD and enables one to reduce the supply voltage; however, these are more complicated to make. When an MCP unit is used to detect single particles, it is desirable that the unit works in saturation, which is characterized by a bell-shaped (quasi-Gaussian) distribution of the output pulses (Fig. 2). The operation of the MCP unit can be characterized by an amplitude resolution R , which is defined as the ratio of the total width at half height ΔA to the most probable pulse height A_m . Typical values of R are 0.6-1.4. The noise-pulse distribution is usually exponential. Therefore, if the saturation state is used there are usually no problems associated with distinguishing the signal from noise by the use of discrimination thresholds in the counting equipment. The MCP unit is brought to saturation by selecting the potential differences applied to the plates U_{p1} and U_{p2} as well as the potential difference ΔU between them. The typical potential difference on a single MCP is 1000 V. The value of ΔU is usually positive, i.e., it accelerates the electrons, and it may be tens or even hundreds of volts. However, ΔU can also be negative (as in [29, 32]), which produces a substantial reduction in K for the unit and a certain reduction in R , i.e., an improvement in the amplitude resolution. The mode of operation is also dependent on the load characteristics: on the total intensity of the flux and on the local flux density at the input surface, because the characteristics deteriorate substantially when the current drawn by the electron avalanches exceeds 10% of the current flowing in the MCP. On the other hand, if avalanches pass too frequently through a given channel in the MCP, they remove charge from the walls, and there will be inadequate

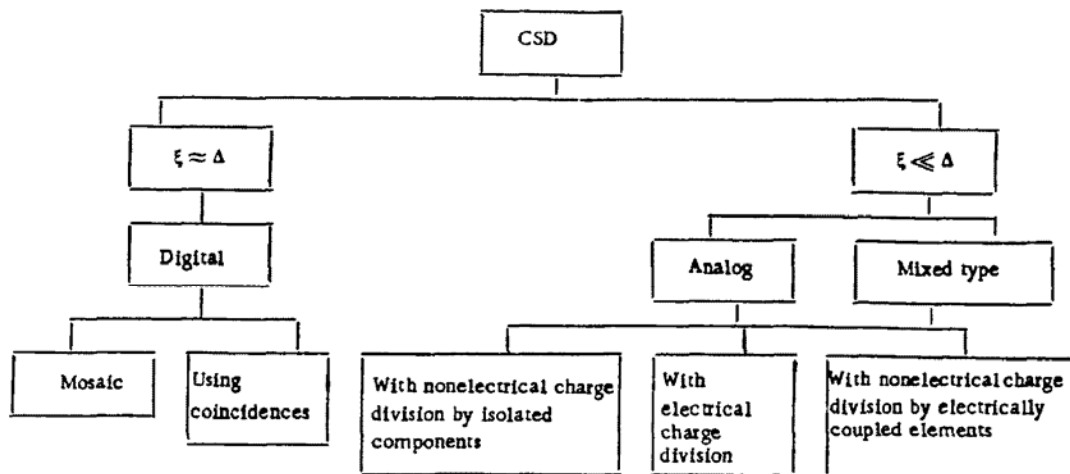


Fig. 3. Main types of CSD.

time for the charge in the conducting wall to recover on account of the low conductivity. The characteristic recovery time is substantially dependent on the design features and mode of operation and may be <10 msec [27, 33, 34].

There is a one-to-one relationship between the coordinates of the electron-avalanche centroid at the output from the second MCP and the coordinates of the channel centers in the input MCP. If the channels are not parallel with respect to the normal to the surface of the MCP, there is a shift identical for all channels (some hundreds of microns) in the centroid with respect to the centers of the corresponding channels. As in most cases one is interested in the relative coordinates rather than the absolute ones, one can identify the coordinates of the centroid at the collector with those of the particle arriving at the detector without introducing an error.

The channel diameters in current MCP are 8–20 μm . It is clearly impossible in principle to determine the coordinates of particle arrival with an accuracy better than the channel size at the input MCP. No matter what the point of arrival within a single channel, the coordinates of the centroid in the electron avalanche will correspond to the center of this channel. The error introduced by the structural discreteness in some cases can be reduced substantially if one has additional information on the flux. This topic has been considered in detail in [35] with reference to the recording of axially symmetrical fluxes.

Another essential constraint on the coordinate measurement accuracy occurs because the electron avalanche whose centroid is used in identifying the coordinates is a statistical object. The mean value of the coordinates for the constituent electrons defines the centroid, while the standard deviation σ_a is determined by the transverse dimension of the avalanche. The resulting centroid position is characterized by a certain distribution around the true position with a standard deviation $\sigma_c = \sigma_a / \sqrt{N_e}$, where N_e is the number of electrons in the avalanche. If K is inadequate, for example 10^5 , and the transverse dimension of the avalanche at the collector is 1 cm, then the error in determining the centroid coordinates due to the statistical character of the avalanche will be $\sigma_c = 10 \mu\text{m}$, which is comparable with the error introduced by the discrete MCP structure.

4. MAIN TYPES OF CSD

CSD are classified in terms of the collector design and the method of deriving the coordinate information. CSD can also be divided into two large groups in terms of spatial resolution. The first group includes CSD whose spatial resolution ξ is approximately equal to the characteristic size of the elements Δ constituting the collector; the second group consists of CSD in which the spatial resolution is substantially less than the characteristic size of these elements. CSD can also be divided into three types by method of determining the coordinates: analog, digital, and mixed (Fig. 3). CSD of digital type constitute the first group; it is in principle impossible to determine the coordinates with an accuracy better than the size of a collector element. CSD of analog and mixed types constitute the second and third groups. In such CSD, one uses avalanche charge division, and the attain-

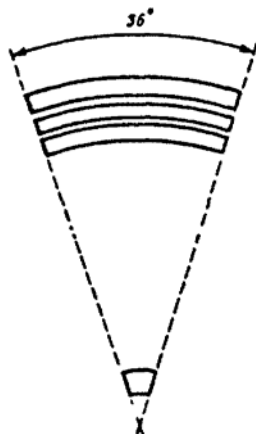


Fig. 4. Mosaic collector with annular sector anodes (only the edge elements in the collector are shown).

able spatial resolution is better by 1-3 orders of magnitude than the characteristic dimensions of the collector elements.

In CSD of digital type, the collector consists of electrically insulated conducting elements (anodes), each of which is connected to its own amplifier, discriminator, and so on. The collector is placed close to the MCP, which prevents the electron avalanche from spreading out. The spread is due in the main to the electrons emerging from the second MCP including ones whose velocities have a substantial component perpendicular to the channel axis [36]. The spread can be reduced by accelerating the electrons by applying a potential difference U_c between the collector and the output from the second MCP (Fig. 1). However, the hazard of electrical breakdown increases with U_c , and the consequences of this may be catastrophic for the electronic components. There are two types of digital CSD: mosaic ones and ones employing coincidence (Fig. 3). In the mosaic type, the electron avalanche falls on one of the anodes, whose signal is directed to the EU, which identifies that collector element. The number of that element in digital form indicates the particle coordinate. If a particle strikes the first MCP in a region lying above the boundary between two adjacent collector elements, there can be pulses in the lines from both such elements. The EU receives the signals from all the anodes and processes the pulses due to a single particle (for example, it rejects such events). The spatial resolution of a CSD of discrete type is equal to the characteristic dimension of a collector element. The shape, size, and number of the anodes in such multianode systems vary considerably and are determined by the purpose. This is illustrated on several examples.

The simplest collector in a mosaic CSD consists of two equal half-circles [23, 37]. A CSD of mosaic type may use collector elements of various shapes, which provides simple solutions to various special problems. For example, in a CSD used to record particles in an experiment with an axially symmetrical distribution [38] one can employ a multianode collector (64 elements) in which the elements are successive ring sectors with an angle of 36° (Fig. 4). The gaps between the anodes are $100 \mu\text{m}$, while the widths vary in such a way that the count rates from the different elements are approximately identical. Such a CSD has a time resolution of 3 nsec.

The designs for two-dimensional CSD include the photomultiplier-CSD (PCSD) [39], which contains a multianode collector composed of 256 (16×16) elements (squares). The proposed size of a collector element is $2.5 \times 2.5 \text{ mm}$, while the insulating gap between elements is $50 \mu\text{m}$. A multianode matrix consisting of 25 (5×5) square anodes has been realized [34]. An analogous CSD with 16 elements has also been described [40]. A substantially more complicated collector consists of 450 needle anodes of diameter 0.3 mm built into a matrix of dimensions $12 \times 16 \text{ mm}$ [41]. The distances between the anodes were 0.7 mm . The anodes were connected to coaxial cables of diameter 0.7 mm . With $U_c = 500 \text{ V}$, a spatial resolution of

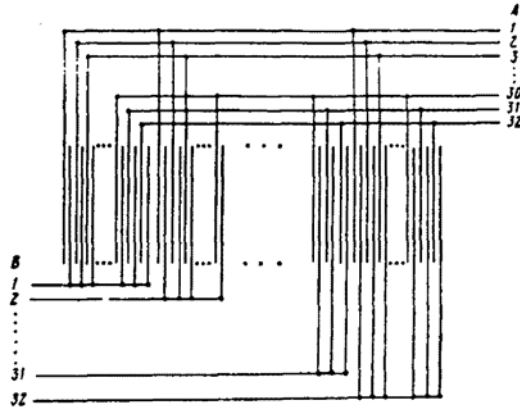


Fig. 5. Collector in a one-dimensional CSD with image resolution into 1024 elements.

0.6 mm was attained. It has been suggested to increase the number of needle anodes to 1205 with a needle diameter of 0.25 mm and a distance between needles of 0.45 mm.

Current microelectronic techniques enable one to manufacture a detector with over 10^3 collector elements per cm^2 . It is also simple to connect an amplifier-discriminator-counter chain to each single anode. However, a system consisting of thousands of such chains would clearly be cumbersome and complicated. It would be a difficult matter to make any changes in this, which conflicts with specifications for laboratory devices.

An alternative approach that substantially reduces the number of electronic units employs coincidence [42]. Very many systems of this type are in use or under development: from simple one-dimensional ones (1×160 or 10×10 elements) to systems consisting of 1×1024 and 1024×1024 elements [43]. The sizes of the collector elements can be reduced to $25 \times 25 \mu\text{m}$, and the elements themselves are mounted on a strong multilayer ceramic substrate. The number of chains is reduced by connecting the anodes in groups in such a way that adjacent elements belong to different groups. If the total number of amplifier-discriminator chains is represented as the sum of two numbers A and B, then such a system enables one to obtain $A \times B$ elements. For example, a system of 1×1024 elements requires only 64 ($32 + 32$) chains. Figure 5 shows an example of such a collector. The elements are divided into 64 groups of two sorts: A and B. The elements in each group are connected together, and each group is connected to an amplifier-discriminator chain. The occurrence of a signal in one of the type B groups enables one to determine the position of the electron avalanche approximately, while the signal from one of the type A groups is used to determine the coordinates exactly. The electron avalanche must necessarily fall on two adjacent elements. Therefore, recording requires the simultaneous occurrence of signals (coincidence) for two groups of elements belonging to different types. Coordinate determination for two-dimensional images is organized similarly. In that case, the collector is a set of insulated strips (rows and columns), and the simultaneous occurrence of signals in one of the columns and one of the rows indicates the avalanche point. The collector groups are of two types: rows and columns in a two-dimensional system. The avalanche may fall on more than two collectors, and this represents interference with binary coincidences, but it can be used in recording and position determination in coincidence for three or even four signals. The MCP gain is high enough for this. If a four-signal coincidence is used in a system with $A \times B \times C \times D$ elements one requires for example $A + B + C + D$ amplifier discriminator chains. Systems of this type are used as a rule in two-dimensional CSD. For example, a detector with 1024×1024 elements requires only 128 ($32 + 32 + 32 + 32$) such chains.

A novel approach to simplifying the electronic system in a multianode unit has been described in [44]. This CSD is used in determining the radial coordinate (distance from the center), with a collector consisting of 50 concentric rings deposited on a glass plate (Fig. 6). The ring width is $100 \mu\text{m}$ and the distance between them is also $100 \mu\text{m}$. The collector elements can be numbered in binary code. The number of amplifiers is equal to the number of bits; each amplifier is put into correspondence with a certain bit. Each of the elements is

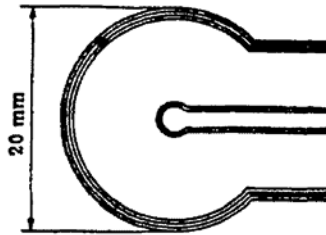


Fig. 6. Collector composed of 50 concentric rings with output leads. Only the edge elements are shown.

connected through a capacitor to the set of amplifiers corresponding to the number of the collector in binary code. For example, collector 7 was connected to amplifiers 1, 2, and 3, while collector 16 was connected only to 5; therefore, an avalanche appearing on a given element produces signals in a certain set of amplifiers. The result is read into the computer (each bit corresponds to a certain amplifier) and indicates the collector element number. An analogous device is a one-dimensional CSD consisting of 1024 elements, which uses only 10 elementary electronic chains and a binary encoding system [45].

A further simplification in the electronics is provided by charge-coupled devices CCD to record the signals: CCD lines and diode lines [46]. An important advantage of collector elements with their own amplifiers, discriminators, and counting devices is that one can record events at different anodes independently. This substantially reduces the dead time and extends the dynamic range up to a count rate of about 10^6 sec^{-1} , which is comparable with the limiting rate for an MCP. Another interesting feature of a digital-type CSD is that one can organize coordinate measurement for several particles arriving simultaneously (a very important problem [4, 47, 48]), which is usually unavailable for charge-division CSD.

This type of CSD also has certain disadvantages. For example, it is impossible to prevent spread in the avalanche completely, which leads to charge appearing on adjacent elements. If the plate has straight channels, it is also not possible to produce an avalanche of width less than $100 \mu\text{m}$ with K of about 10^7 (and correspondingly this spatial resolution). Differences in the thresholds in the amplifier-discriminator chains lead to the recording efficiency being dependent on the coordinate. The capacitive coupling also increases as the size of the collector elements decreases. The elimination of spurious coincidences substantially complicates the coordinate-determination circuit, particularly when one uses three or four signals in coincidence. Also, in spite of the use of coincidence, the volume of electronic equipment remains considerable: hundreds of elementary chains.

Analog type CSD can provide a spatial resolution substantially less than the dimensions of a collector element. They can be divided into three groups (Fig. 3). In CSD with non-electrical charge division by insulated collector elements, the avalanche falls on several metal collector elements, each of which is connected to its own charge-sensitive amplifier. The charge will be distributed between the elements in a way dependent on the position of the avalanche center. One measures the charges on all the elements and uses an appropriate algorithm to determine the centroid coordinates and correspondingly those of the input particle. A major feature of this type of CSD is that the charge division is determined by the collector geometry. In a CSD with electrical charge division, the avalanche falls on a single large collector made of semiconducting material (resistive anode) with several outputs, in which the signals (charge or time) are dependent on the coordinates. In a CSD with non-electrical division of the charge by elements with electrical connection, the avalanche falls on a system of metal collector elements connected together by resistors or capacitors. The number of leads from such a system is less by an order of magnitude than the number of elements. Here also the signals on the collector leads are dependent on the avalanche position.

The first CSD with nonelectrical charge division were ones with quadrant anodes [44, 49], where the collector consists of four circular sectors or quadrants (Fig. 7), each of which is connected to a charge-sensitive amplifier and then to a system for centroid coordinate determination. If q_1, q_2, q_3, q_4 are the charges falling on the corresponding elements, the coordinates of the centroid are defined by

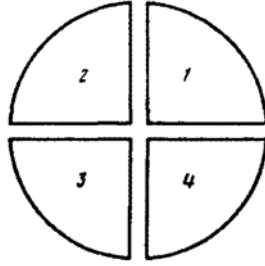


Fig. 7. Anode of quadrant type.

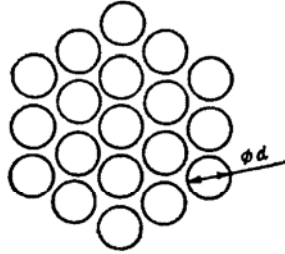


Fig. 8. Collector composed of 19 anodes forming a hexagonal structure.

$$X = K(X, Y)(q_1 + q_4 - q_3 - q_2)/q_0,$$

$$Y = K(Y, X)(q_1 + q_2 - q_3 - q_4)/q_0,$$

where $q_0 = q_1 + q_2 + q_3 + q_4$ (note that X and Y are independent of the absolute value of q_0). The coefficient K is a scale factor and is dependent on the density distribution in the avalanche and incorporates the nonlinearity in the device. For the case of a Gaussian distribution, an exact analytical relationship has been derived between X and Y on the one hand and the charges on the quadrants on the other [50]. If $K = \text{const}$ (i.e., the charges q_i are linearly dependent on the coordinates), the algorithm for deriving X and Y can be realized in a simple analog fashion. If one specifies some density distribution in the avalanche, such as a Gaussian one, it can be shown simply that K is only slightly dependent on X and Y at the center of the collector in a region whose size is not a very large fraction of the standard deviation σ of the avalanche width. This is confirmed by experiment. For example, if $D = 16 \text{ mm}$ is the distance between the MCP and the collector and $U_c = 0$ (Fig. 1), there was no distortion in the image on the assumption that $K = \text{const}$ for a field of view of diameter 3 mm [49]. A resolution of $50 \mu\text{m}$ was obtained with $U_c = 50 \text{ V}$. A resolution better than $25 \mu\text{m}$ was attained by reducing D to 0.5 mm . In another detector, the linearity region was 1 mm with a size of the avalanche at the collector of $\sigma = 10 \text{ mm}$, $D = 2.2 \text{ mm}$, while the resolution near the center was $50 \mu\text{m}$ [44].

The resolution of a CSD with nonelectrical charge division by insulated elements is determined by the size of the channels in the first MCP and by the inherent noise in the charge-sensitive amplifiers, which can be made extremely small, as well as by the spread in the charges falling on the elements (this is unimportant for a CSD with a quadrant anode [50]), with a further effect from the noise in the electronic circuits that determine X and Y from q_i . A study of these factors has shown that such a CSD in principle provides a resolution of about 1000×1000 image elements [51].

The collector system is easy to manufacture and the electronic circuit is simple, which are major advantages of CSD with a quadrant anode [50]. The main difficulties with such CSD are due to the nonlinearity, which increases from the center to the edge. The linearity zone is restricted to a few millimeters, which means that the facilities of the MCP cannot be fully used. One can correct for the CSD nonlinearity, i.e., the coefficient K , either by analog means in real time, which clearly is very complicated, or else during subsequent image processing. The processing is not complicated if the correction coefficient can be

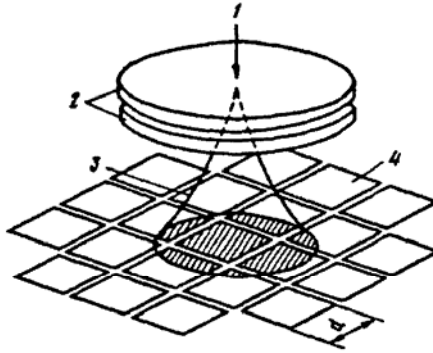


Fig. 9. CSD with collector consisting of 21 square anodes: 1) input particle; 2) MCP unit; 3) electron avalanche; 4) collector elements.

represented as the product of two cofactors, each of which is dependent on only one of the coordinates. If this is not so, recovery of the true image is greatly complicated.

The above arguments show that it is necessary to devise other ways of extending the linearity zone for such CSD. We now consider one method. In a one-dimensional detector, the exact position of the center of gravity is defined by

$$X_g = \frac{\int q(X) X dX}{\int q(X) dX}, \quad (1)$$

where $q(X)$ is the charge density distribution along the X coordinate. For a collector in the form of a set of anodes, one can determine the quantity

$$X_g^* = \frac{\sum f_i q_i}{\sum q_i}, \quad (2)$$

where f_i is the coordinate of the center in element i and q_i is the charge it receives; the summation is taken over all elements. Here X_g^* is analogous to X_g and becomes the ratio of the integrals of (1) in the limit of indefinite reduction in element size and increase in the number. If the number of collectors is limited, the determination of the coordinate from (2) is not accurate and is a reason for nonlinearity. The collector systems in CSD of this type may consist for example of circular or hexagonal elements forming a hexagonal structure (Fig. 8) [52, 53], similar to those used in scintillation PSD [54, 55]. A CSD has been described having a collector consisting of a matrix of square elements in which the corner ones are missing (Fig. 9) [56, 57]. The use of 19 or 21 amplifiers somewhat complicates the electronic circuit, but it provides good characteristics over the entire input surface. For example, for the collector shown in Fig. 8 with an avalanche of size $\sigma \approx 1.5d$ (diameter of collector element $d = 9$ mm) a resolution of $\approx 80 \mu\text{m}$ was attained, and the image distortion was slight.

The most interesting and promising method requires three or four amplifiers together with a simple circuit for adding and dividing the charges and a collector system in the form of wedges and bands [54]. Figure 10 shows part of the collector system in such a CSD. The collector elements are connected in four groups (A, B, C, and D) and each of these is connected to a charge-sensitive amplifier. The width of the bands A and B (C and D) decreases (increases) linearly as the Y (X) coordinate changes. The coordinates are determined as

$$X = Q_C / (Q_C + Q_D); \quad Y = Q_A / (Q_A + Q_B).$$

One such collector system made by photolithography had dimensions 2.5×2.5 cm and consisted of 17 quartets A, B, C, and D with a period of 1.5 mm [51]. The conducting elements were separated by insulating gaps of width 30 μm . The avalanche falls on two or three such quartets. A resolution better than 50 μm was attained, while the distortion was slight. The cartesian or polar coordinates of the input particles can be determined by means of collector elements connected in only three groups [51]. For such a collector (Fig. 11), the Cartesian coordinates are defined as $X = 2Q_A/Q_0$, $Y = 2Q_B/Q_0$, where $Q_0 = Q_A + Q_B + Q_C$. The widths of the strips A and of the central zigzag C varied linearly with the X coordinate. In this system, the collector elements of one type are connected together and it is not necessary to

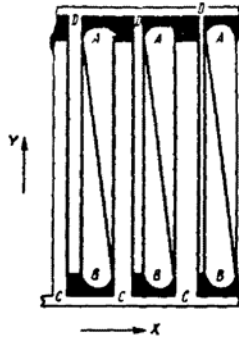


Fig. 10. Collector in the form of wedges and strips combined into four groups.

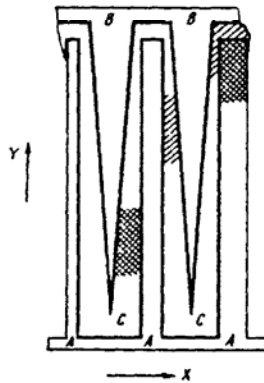


Fig. 11. Collector in the form of wedges and strips combined into three groups.

have leads for all the A and B wedges through the substrate, in contrast to the case shown in Fig. 10. To record an image in the visible wavelength range by means of this collector system, a LCSD was built providing a high resolution (down to $30 \mu\text{m}$) and good linearity [58, 59]. Such devices in fact are electron-optical converters with digital image readout.

Electron-beam lithography can be used to make collectors in the form of wedges and bands to provide accuracy in the elements better than $1 \mu\text{m}$ [60]. It is possible to make collectors with any variation in the widths of the strips and wedges, e.g., logarithmic or stepped. This produces an output signal functionally dependent on the coordinates. For example, a collector has been described [60] providing directly a signal proportional to the square of the distance from the center of the CSD, which was intended for use in a Fabry-Pérot interferometer. Also, in this way one can correct some distortions (aberrations) introduced by the system for forming the image at the CSD input. A CSD with collector elements in the form of wedges and strips has good linearity and resolution up to 1000×1000 elements, while the manufacture is relatively simple, and the operation requires uncomplicated circuits.

In a CSD with electrical charge division, the collector (resistive anode) is a plate with distributed resistance, capacitance, and inductance, whose shape and size are determined by the use. The production technology has been briefly discussed in [61]. The charge reaching the plate is divided between two or four leads at the edges in the one-dimensional and two-dimensional cases. The characteristics of a system with a resistive anode have been considered [61, 62].

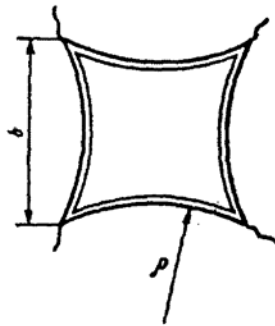


Fig. 12. Collector as a resistive anode with four leads; $b = 29$ mm, $\rho = 58$ mm.

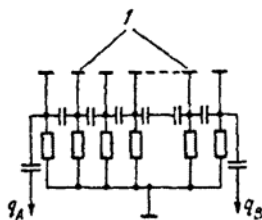


Fig. 13. One-dimensional collector composed of 20 parallel wires linked by capacitors; all the capacitors are 100 pF, while all the resistors are 2.7 MΩ.

Detailed consideration of the charge division in the one-dimensional case indicates that this occurs in accordance with the ratio of the resistances between the point of injection and the leads, and it is independent of the resistance of the line between the leads, the signal propagation mechanism, and the capacitance and inductance distribution along the line [63]. The finite size of the electron cloud does not restrict the resolution, since this is determined by the position of the centroid. A resistive anode has a distributed capacitance, so the signal rise times at the leads will be dependent on the injection position. There are two ways of determining the coordinates: by measuring the total charges at the leads and from the pulse shape. Both are applicable to the one-dimensional and two-dimensional cases. There is a discussion [61] of possible ways of realizing these two methods (in all there are 11 circuits) and the characteristics of these. Some general specifications can also be drawn up for the electronic circuit [62]. For example, when the charges at the leads are used, the anode time constant should be small by comparison with the time constants of the charge-sensitive amplifiers in order to minimize the nonlinearity arising from variations in pulse shape. If the rise time is used, the anode time constant should be comparable with those in the amplifiers.

The simplicity of this type of CSD is one of its main advantages. However, the spatial resolution is restricted by the noise current at the amplifier inputs, whose source is thermal fluctuations, which in units equivalent to the charge constitute $Q_N = (4kT\tau/r)^{1/2}$, where r is anode resistance, τ is amplifier time constant, k is Boltzmann's constant, and T is temperature [61]. The charge fluctuations increase as r decreases, while when it is increased the pulses are heavily attenuated and rise slowly. The optimum anode resistance is approximately equal to τ/C , where C is anode capacitance; then the noise will be equal to the equivalent charge $Q_N = 2(kTC)^{1/2}$. The CSD resolution is determined by Q_N and usually to raise the resolution one has to increase K , sometimes by the use of complicated structures such as a block of five MCP [32].

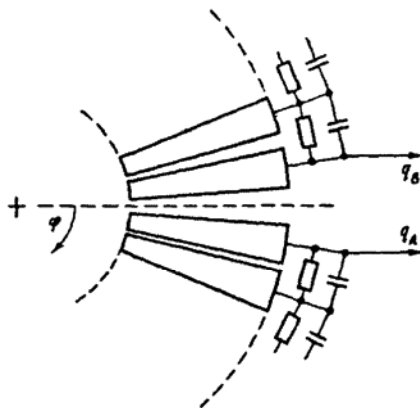


Fig. 14. Collector consisting of 39 elements forming parts of a ring.

One-dimensional detectors [64-67] and two-dimensional ones [32, 62, 68-71] are widely used; as an example we may note a one-dimensional CSD in which a strip of length 18 mm provided a resolution of 18 μm with good linearity [19], another example being a two-dimensional CSD in which the resistive anode was a square plate of size 6.5 \times 6.5 cm with four leads at the corners [61].

All the two-dimensional systems that have been described have nonlinearity increasing away from the center, which produces appreciable distortion. A method has been described [72] for producing a resistive anode without distortion. The basis of the correction is provided by [73], which implies that a current flowing uniformly over an infinite plane with resistance r_{\square} is not perturbed by a circular hole of radius a if this hole has a linear resistance $R_l = r_{\square}/a$ along its boundary. This effect applies also for an anode of finite dimensions whose boundaries are represented by concave parts of circles. Such an anode (Fig. 12) has been used in a CSD [62]. The anode was at 1 mm from an MCP with $U_c = 200$ V. The system was linear throughout the input detector area of diameter 25 mm and the resolution was not worse than 200 μm . Such a collector is very interesting and not very complicated to make; it has been used in many CSD, for example in the PCSD of [69-71] and has even been manufactured commercially [32, 74]. However, to obtain a resolution of 30-50 μm requires $K \approx 10^7$ - 10^8 , which requires high MCP voltages and thus reduces their working life. At count rates $\geq 10^4$ - 10^5 sec^{-1} , a CSD with a resistive anode is substantially inferior in characteristics to a CSD with nonelectrical charge division [58].

In the analog CSD of the third group, the collector consists of insulated metal elements connected together electrically by means of resistors or capacitors. The first charge-division CSD appear to have been of this type [75]. The working principle is closely illustrated by a one-dimensional collector [76]. This consisted of 20 parallel stretched wires of diameter 100 μm (Fig. 13) linked by capacitors $C = 100$ pF each. Two charge-sensitive amplifiers were connected to the ends of this chain. When an avalanche with charge q_0 fell on the collector, the amplifiers received charges q_A and q_B , and there are no losses if C is substantially larger than the parasitic capacitance and $q_0 = q_A + q_B$; if the charge falls on wire n out of N wires, then $q_A/q_0 = n/N$. Note that this expression is independent of q_0 . If on the other hand C is comparable with the parasitic capacitance, the sum of the charges collected at the ends of the chain will be less than q_0 and nonlinearity occurs. However, the noise increases with C , so a compromise must be found in each particular case. It has been shown also in [76] that if the avalanche falls simultaneously on several elements, the system determines the center of gravity. Also, this spread is desirable, because it reduces the nonlinearity. This collector system provided a resolution of 75 μm with satisfactory linearity on a strip of length 4 mm. The errors introduced by the noise into the coordinate determination in such systems have been considered [77]. In [76], there is a discussion of the scope for constructing a two-dimensional system, and a prototype with a collector composed of 7×7 elements was described. Such a collector system is complicated to manufacture, but the elements are all of the same type, so it might be possible to use thin-film technology.

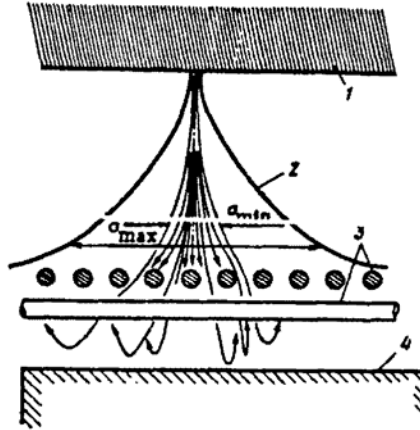


Fig. 15. Two-dimensional CSD of mixed type: 1) output from second MCP; 2) electron avalanche; 3) two orthogonal sets of parallel wires as anodes; 4) reflecting electrode; $\sigma_{\max} = 2 \text{ mm}$, $\sigma_{\min} = 0.5 \text{ mm}$.

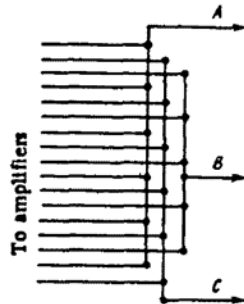


Fig. 16. Scheme for linking amplifiers in CSD with multiwire collector.

A one-dimensional detector is described in [78] for determining angular coordinates, which uses this principle. The collector consists of 39 strips on a ceramic substrate, which are equal parts of a ring (Fig. 14). The collector elements are connected together by 800 pF capacitors. Two amplifiers measure the charges arriving at the ends. The angular coordinate is determined as $\varphi = 2\pi h(X)$, where $X = q_A/(q_A + q_B)$, and h is a function of X , and in the ideal (linear) case $h(X) = X$. The parasitic capacitances however result in some non-linearity, which can be eliminated on processing by fitting a polynomial of third degree to $h(X)$. The processing time for one event with a microprocessor is 100 μsec . The determination of the radial coordinate is similar for the collector shown in Fig. 6 [44], where there are 31 concentric rings. The rings are connected by 1500-pF capacitors; the signal from each tenth ring was taken to an amplifier and then to the coordinate-determination system. The use of four output points instead of two slightly complicates the algorithm but improves the linearity and resolution. The collector elements may be linked by resistors instead of capacitors, as for example in [21].

In CSD of mixed type, the region where the particle enters is determined by the discrete method, while the exact coordinates within this region are determined by the analog method from the charge division. A CSD of this type has been used in the x-ray telescope in the HEAO-B space high-energy astrophysical observatory (USA) and has record characteristics [11, 79]. The electron-avalanche detector in the CSD is provided by two orthogonal grids consisting of parallel wires of diameter 100 μm (Fig. 15). The distance between wire centers is 200 μm ; the distance between the grids is also 200 μm . The wires are joined to adjacent

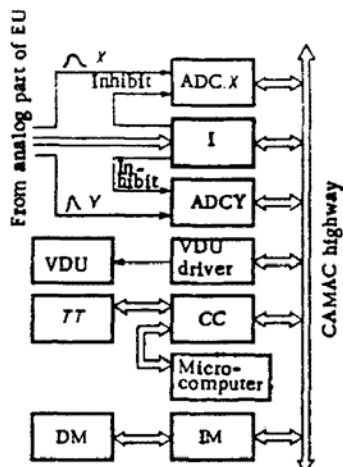


Fig. 17. Block diagram of system for receiving and processing signals from CSD based on CAMAC modules and a microcomputer: VDU visual display unit; TT teletype; DM disk memory; I interface; CC crate controller; IM interface module.

ones by 10-k Ω resistors. The voltages on the grids and on the reflecting electrode at a distance of 250 μm are chosen such that the avalanche charge is divided approximately equally between the grids. The avalanche diameter ranges from 0.5 to 2 mm, and the position of the centroid is determined independently from the signals from the two grids. (We note that a similar one-dimensional system [76] has been considered above.) An amplifier is connected to each eighth wire. There were 34 amplifiers, with 17 on each grid (coordinate). These amplifiers were joined into three groups: A, B, and C, as shown in Fig. 16. The exact position of the centroid was determined from the charge division between these three groups, for example as $(Q_A - Q_C)/(Q_A + Q_B + Q_C)$. Each amplifier had an additional output to a system for determining the coordinates approximately, which indicates the region where the avalanche occurred. The characteristics of the circuit elements have been described in detail [80]. The CSD provides high linearity and resolution down to 10 μm over an area of 26 \times 26 mm, which corresponds to $6 \cdot 10^6$ image elements. It has been pointed out [11] that the resolution is determined by the unit that derives the coordinates exactly and does not deteriorate on increasing the area, and correspondingly the numbers of wires and amplifiers. The detector also enables one to select events by amplitude and to exclude events corresponding to the simultaneous arrival of two particles. The electronic circuit in this CSD was designed to record very weak fluxes (100 particles/sec).

This CSD was used in a detector with a photocathode placed ahead of the MCP together with an electrostatic lens system [81]. This PCSD enables one to record and determine the coordinates of photons in the wavelength range 1200–7300 \AA in accordance with the type of photocathode. In a fast PCSD similar to that described above, there were nine amplifiers connected to each grid in the multiwire collector [82]. The PCSD provided a resolution of 30 μm over a field of diameter 25 mm and could handle count rates up to $6 \cdot 10^4 \text{ sec}^{-1}$ with a background count rate of 50 sec^{-1} . It may be noted that it is not essential to arrange the amplifiers connected to the wires in three groups. A comparison has been made [83] of various amplifier grouping systems and their effects on the noise in systems containing wire collectors, together with the effects of parasitic capacitances.

Mixed-type CSD combine unique resolution and linearity, but they are relatively complicated. It is difficult to provide a uniform distribution for a large number of wires in the collector. Resistors for charge division increase the noise. The electronic circuit is also fairly complicated.

5. CSD ELECTRONIC SYSTEMS

Standard laboratory units are employed to derive the coordinate information from the CSD signals: charge-sensitive amplifiers, shapers, discriminators, scalars, division circuits, time-to-amplitude converters, analog-digital and digital-analog converters (ADC and DAC), and so on. There is therefore no need to consider the characteristics of the individual units, and we merely note that the specifications for these arising from the specific features of CSD have been discussed in detail in [2]. We consider only some general specifications for the systems for receiving the CSD signals.

Preprocessing usually amounts to two operations: displaying the image on a storage oscilloscope or TV display and performing various transformations on the coordinates. If further image processing is required, the image may be stored in the computer memory, in special random-access memory units, or on magnetic media. A computer should be a component part of EU (often a microcomputer is sufficient). If one uses a specialized CSD to handle a strictly defined problem with well-known ranges and modes of operation and signal-selection conditions, then it is preferable to employ a specialized processes with a preset program and to realize some of the operations by hardware. This provides an improvement in processing speed. If on the other hand one is commissioning and testing CSD or using them under conditions where the modes of operation and signal-selection requirements and processing vary considerably, as is common in physics laboratories, then it is desirable to use an unspecialized computer with high-level programming languages and to give preference to software processing, although this involves some loss of processing speed.

In digital CSD, the coordinates are determined directly in digital form, and therefore it is necessary to use a DAC to produce the control signals for display for example on a storage oscilloscope. In an analog CSD, one determines the signal time differences or the charge division as a rule by analog means, and the coordinate signals are presented as pulses with amplitudes proportional to the corresponding coordinates. In that case one does not need a DAC to display the image, but ADC are required for digitization. The design of fast ADC is developing rapidly; in charge-division CSD, it is possible to measure signals from each collector element with the required accuracy and determine the coordinates in digital form. This improves the noise immunity and the image recovery accuracy.

Figure 17 shows an example of the processing unit for use with a CSD to provide coordinate information by means of a microcomputer and a CAMAC system [52, 53, 56, 57]. The two ADC in the analog part of the EU receive pulses with amplitudes proportional to X and Y, while a special interface records logic signals indicating particle recording and selection. When the interface receives a signal that a particle has been recorded, the ADC inputs are gated and the microprocessor handles the event: It takes the ADC readings and clears the latter, reads the logic signals in the interface, performs the necessary transformations on the coordinates, writes them to disk, and brightens up the corresponding point on the VDU, etc. Then the inputs to the interface and the ADC are activated again and the system can process the next event.

6. EXAMINATION OF CSD CHARACTERISTICS

It is fairly complicated to test CSD, i.e., to determine the resolution, distortion, dynamic range, and so on. Many different criteria can be used to evaluate performance such as have been developed for evaluating optical systems [84].

Two ways of testing CSD can be distinguished. In one of them, the CSD records a point particle or photon beam, i.e., a beam whose transverse dimension is much less than the CSD spatial resolution. It should be possible to scan the beam with high spatial accuracy over the input surface. The resolution is determined from the image of the beam. One can compare given beam displacements with image displacements as for example in [44] to identify the distortions, i.e., the nonlinearity. The second test method is analogous to one widely used in optics and consists in imaging masks [11, 32, 49, 51, 58, 61, 62, 71, 82]. The mask may be for example a narrow slit illuminated by ultraviolet light placed in front of the CSD [52, 53]. The resolution (75 μm) is determined from the slit width. The standard deviation of the slit image from a straight line (120 μm) characterizes the nonlinearity. The occurrence of additional distortion as the count rate increases enables one to determine the limiting count rate.

7. CSD APPLICATIONS

Promising uses have been noted above. At present, CSD are widely used in space experiments to record ultraviolet radiation [3, 43, 45, 46, 65, 57] and x rays [3, 11, 85]. CSD are also used in ultraviolet spectrometers carried on research rockets, which has provided for measuring the spectra of weak astronomical sources, while CSD may also be used to record images in the focal plane of an x-ray telescope, which has been so successful [86] that almost all launches of x-ray telescopes planned for the 1980s [85, 87-91] will use CSD, as will a telescope for hard ultraviolet radiation [92, 93]. PCSD have also been produced for recording photons in the visible range [32, 58, 68-71, 94]. PCSD have also been used in Cherenkov counters, as well as in ground optical astronomy [94], where they have larger dynamic ranges than CCD matrices in recording weak fluxes [81]. For example, PCSD have been used as image recorders (electronic plates) in various telescopes [43, 68], including the 2-m telescope in Mexico. PCSD also enable one to record time variations in luminosity and to recover images with high resolution by interference methods [95]. Only avalanche-diode matrices [96, 97] are likely to compete with PCSD in the future [6, 94].

CSD are also widely used in laboratory experiments. For example, they are employed in mass spectrometry to improve the resolution and sensitivity as well as the measurement rate, particularly in isotope analysis [64]. They enable one to record a wide energy range for electrons in energy analyzers simultaneously [98, 99] and reduce by two orders of magnitude the measurement time in thin-foil spectroscopy [66]. Their use in surface research [78, 100] has provided increased speed and accuracy, with considerable reductions in the intensity of the probe fluxes. CSD are also widely used in experiments in electron and atomic collision physics [4]. A large time advantage occurs in the measurement of differential electron scattering [44]. CSD are also used in research on high-energy differential ion and neutral-particle scattering to improve the angular resolution, sensitivity, and accuracy, which has enabled the observation of diffraction effects and has reduced the measurement time by more than an order of magnitude [101]. CSD have also improved the performance in measuring differential scattering accompanied by photon emission [38, 40] and have reduced the time required by 3-4 orders of magnitude in experiments on molecular disintegration in collisions [18]. In nuclear physics, CSD are used as start-pulse generators to determine the point of entry of a high-energy particle into a foil, which has eliminated errors in measuring times of flight associated with uncertainty over particle paths [21, 102].

8. CONCLUSIONS

Although CSD open up new possibilities, the examples of their use at present are not numerous, which is due to various factors, particularly the need to make various components oneself, including the electronic parts, as well as the need to use computers operating in real time to accumulate and process the large data volumes that inevitably arise in image processing. However, automation in physics experiments is a characteristic current trend. More and more laboratories are being equipped with their own minicomputers and microcomputers such as the Elektronika-60 [103], and they are accumulating experience in automating experiments.

Of the various types of CSD, the most promising for users and also the least complicated are the discrete and the type with the collector in the form of wedges and strips. The discrete type is preferable when one requires a moderate resolution and it is necessary to record high fluxes (10^3 - 10^6 sec^{-1}) or to record several particles arriving simultaneously. It is true that the latter task can be handled by especial-design analog CSD [18]. When high resolution is required (about 20-30 μm) and the limiting count rates are $\leq 10^4$ - 10^5 sec^{-1} , it is preferable to use a CSD with the collector in the form of wedges and strips. Such a collector can readily be made by photolithography; also, the electronic circuits are relatively simple: 3-4 charge-sensitive amplifiers and ADC, which are commercially available, for example in the form of modules in the CAMAC standard. Also, an MCP unit is commercially available: the VEU-7 [104], which has characteristics corresponding to those required for CSD. This enables one to build CSD under laboratory conditions from standard units with the minimum number of especially made devices. Such CSD have adequate characteristics, although not unique ones. Therefore, the basis exists for the general use of CSD in laboratory physics research in various areas, particularly where the particle is an electron or can produce a secondary electron. This applies particularly to nuclear physics, the physics of electron and atomic collisions, optics, mass spectrometry, electron microscopy, x-ray analysis, and surface examination.

The author is indebted to V. B. Leonas, who aroused his interest in CSD based on MCP, for support and interest in the work and for fruitful discussion of problems connected with CSD.

LITERATURE CITED

1. V. P. Kleimenov, Yu. N. Koblik, V. N. Kuz'min, and B. S. Mazitov, Coordinate-Sensitive Detectors [in Russian], FAN, Tashkent (1979).
2. L. S. Gorn and B. I. Khazanov, Position-Sensitive Detectors [in Russian], Énergoizdat, Moscow (1982).
3. M. Lampton, Proc. Intern. Astron. Union Colloq. 40, Meudon Observ., France (1977), p. 32/1.
4. R. W. Wigjaendts van Resandt and J. Los, Proc. XI Intern. Conf. on Physics of Electron and Atom. Collisions, North-Holland Publishing Co., The Netherlands (1980), p. 831.
5. M. Lampton, Sci. Amer., 245, No. 5, 62 (1981).
6. M. A. Gruntman, Preprint IKI Akad. Nauk SSSR, No. 701, Moscow (1982).
7. V. N. Bragin and A. E. Melamud, in: Surveys of Science and Engineering: Electronics and Its Applications [in Russian], VINITI, Moscow (1977), Vol. 9, p. 102.
8. J. Freeman, S. Bower, F. Paresce, and M. Lampton, Rev. Sci. Instrum., 47, No. 3, 277 (1976).
9. C. I. Coleman, Appl. Opt., 20, No. 21, 3693 (1981).
10. M. R. Ainbund and V. Ya. Zaslavskii, Prib. Tekh. Eksp., No. 4, 181 (1975).
11. E. Kellog, P. Henry, S. Murray, et al., Rev. Sci. Instrum., 47, No. 3, 282 (1976).
12. W. E. Baumgartner and W. K. Huber, J. Phys. E, 9, No. 5, 321 (1976).
13. J. O. Olsen, J. Phys. E, 12, No. 11, 1106 (1979).
14. D. H. Ceckowski, E. Eberhardt, and E. Carney, IEEE Trans., NS-28, No. 1, 667 (1981).
15. J. G. Timothy, Rev. Sci. Instrum., 52, No. 8, 1131 (1981).
16. P. Hvelplund, E. Laegsbaard, and E. H. Pedersen, Nucl. Instrum. Methods, 101, No. 3, 497 (1972).
17. K. Kuroda, D. Sillou, and F. Takeutchi, Rev. Sci. Instrum., 52, No. 3, 337 (1981).
18. D. P. De Bruijn and J. Los, Rev. Sci. Instrum., 53, No. 7, 1020 (1982).
19. W. Parkes, K. D. Evans, and E. Mathieson, Nucl. Instrum. Methods, 121, No. 1, 151 (1974).
20. R. W. Winhaendts van Resandt, C. de Vreugd, R. L. Champion, and J. Los, Chem. Phys., 26, 223 (1977).
21. A. M. Zebelman, W. G. Meier, K. Halbach, et al., Nucl. Instrum. Methods, 141, No. 3, 439 (1977).
22. F. Busch, W. Pfeffer, B. Kohlmeier, et al., Nucl. Instrum. Methods, 171, No. 1, 71 (1980).
23. M. A. Gruntman and V. A. Morozov, Preprint IKI Akad. Nauk SSSR, No. 667, Moscow (1981).
24. D. Washington, V. Duchenois, R. Polaert, and R. M. Beasley, Acta Electronica, 14, No. 2, 201 (1971).
25. B. Lescovar, Phys. Today, 30, No. 11, 42 (1977).
26. B. Lecomte and V. Perez-Mendez, IEEE Trans., NS-25, No. 2, 964 (1978).
27. J. L. Wiza, Nucl. Instrum. Methods, 162, No. 1-3, Part 2, 587 (1979).
28. S. Dhawan, IEEE Trans., NS-28, No. 1, 672 (1981).
29. M. R. Ainbund and B. V. Polenov, Secondary-Electron Multipliers of Open Type and Their Applications [in Russian], Énergoizdat, Moscow (1981).
30. V. D. Dmitriev, S. M. Luk'yakov, Yu. E. Penionzhkevich, and D. K. Sattarov, Prib. Tekh. Eksp., No. 2, 7 (1982).
31. D. P. De Bruijn, P. van Deenen, D. Dijkamp, et al., Microchannel Plate Report, edited by H. Hersten, FOM-Inst. voor Atoom- en Molecuulfysica, The Netherlands (1982), Chap. 1.
32. C. Firmani, E. Ruiz, C. W. Carlson, et al., Rev. Sci. Instrum., 53, No. 5, 570 (1982).
33. S. Dhawan and R. Majka, IEEE Trans., NS-24, No. 1, 270 (1977).
34. G. Pietri, IEEE Trans., NS-24, No. 1, 228 (1977).
35. M. A. Gruntman, J. Phys. E., 13, No. 4, 388 (1980).
36. N. P. Zanodvorov, N. K. Zolgina, A. M. Tyutikov, and Yu. A. Flegontov, Radiotekh. Elektron., 25, No. 8, 1745 (1980).
37. M. A. Gruntman and V. A. Morozov, J. Phys. E., 15, No. 12, 1356 (1982).
38. J. C. Brenot, J. A. Fayeton, and J. C. Houver, Rev. Sci. Instrum., 51, No. 12, 1623 (1980).

39. J.-P. Boutot and J.-C. Delmotte, *L'Onde Electrique*, 56, No. 2, 59 (1976).
40. J. Hermann, B. Menner, E. Reischer, et al., *J. Phys. B*, 13, No. 5, L165 (1980).
41. K. Oba, M. Sugiyama, Y. Suzuki, and Y. Yoshimura, *IEEE Trans.*, NS-26, No. 1, 346 (1979).
42. J. G. Timothy and R. L. Bybee, *Rev. Sci. Instrum.*, 46, No. 12, 1615 (1975).
43. J. G. Timothy, G. H. Mount, and R. L. Bybee, *IEEE Trans.*, NS-28, No. 1, 689 (1981).
44. R. W. Wijnaendts van Resandt, H. C. den Harink, and J. Los, *J. Phys. E*, 9, No. 6, 503 (1976).
45. W. E. McClintock, C. A. Barth, R. E. Steele, et al., *Appl. Opt.*, 21, No. 17, 3071 (1982).
46. A. L. Broadfoot and B. R. Sandel, *Appl. Opt.*, 16, No. 6, 1533 (1977).
47. M. J. Gaillard, Abstracts VIII Intern. Symp. on Molecular Beams, Univ. Nice, France (1981), p. 166.
48. M. Algranati, A. Faibis, R. Kaim, and Z. Vager, *Nucl. Instrum. Methods*, 194, No. 2, 303 (1982).
49. M. Lampton and R. F. Malina, *Rev. Sci. Instrum.*, 47, No. 11, 1360 (1976).
50. E. Mathieson, *J. Phys. E*, 12, No. 3, 183 (1979).
51. C. Martin, P. Jelinsky, M. Lampton, et al., *Rev. Sci. Instrum.*, 52, No. 7, 1067 (1981).
52. M. R. Ainbund, L. S. Gorn, M. A. Gruntman, et al., Preprint IKI Akad. Nauk SSSR, No. 787, Moscow (1983).
53. M. R. Ainbund, L. S. Gorn, M. A. Gruntman, et al., *Prib. Tekh. Eksp.*, No. 1, 70 (1984).
54. H. O. Anger, *Trans. Instrum. Soc. Amer.*, 5, No. 4, 311 (1966).
55. A. N. Varin, S. D. Kalashnikov, and V. L. Krivoshein, *Applied Nuclear Spectroscopy* [in Russian], Atomizdat, Moscow (1979), Issue 9, p. 26.
56. L. S. Gorn, M. A. Gruntman, D. S. Zakharov, et al., Abstracts for the Third International Conference of the Socialist Countries on Scientific Space Instrumentation [in Russian], IDI Akad. Nauk SSSR, Moscow (1982), p. 57.
57. L. S. Gorn, M. A. Gruntman, D. S. Zakharov, et al., *Scientific Space Instrumentation: Instruments for Examining Plasma and Electromagnetic Fields* [in Russian], Metallurgiya, Moscow (1983), p. 82.
58. D. Rees, I. McWhirter, A. H. Greenaway, et al., *J. Phys. E*, 16, No. 4, 391 (1983).
59. O. H. W. Siegmund, S. Clothier, J. Thornton, et al., *IEEE Trans.*, NS-30, No. 1, 503 (1982).
60. W. M. Burton, *J. Phys. E*, 16, No. 4, 407 (1983).
61. M. Lampton and F. Paresce, *Rev. Sci. Instrum.*, 45, No. 9, 1098 (1974).
62. M. Lampton and C. W. Carlson, *Rev. Sci. Instrum.*, 50, No. 9, 1093 (1979).
63. V. Radeka and P. Rehak, *IEEE Trans.*, NS-26, No. 1, 225 (1979).
64. V. I. Dukhanov, A. G. Zelenkov, A. A. Kurashov, et al., *Prib. Tekh. Eksp.*, No. 3, 170 (1980).
65. S. Bower, R. Kimble, F. Paresce, et al., *Appl. Opt.*, 20, No. 3, 477 (1981).
66. B. M. Johnson, K. W. Jones, D. C. Gregory, et al., *Phys. Lett.*, 86-A, No. 5, 285 (1981).
67. G. F. Hartig, W. G. Fastie, and A. F. Davidsen, *Appl. Opt.*, 19, No. 5, 729 (1980).
68. L. Mertz, T. D. Tarbell, and A. Title, *Appl. Opt.*, 21, No. 4, 628 (1982).
69. D. Rees, I. McWhirter, P. A. Rounce, et al., *J. Phys. E*, 13, No. 7, 763 (1980).
70. D. Rees, I. McWhirter, P. A. Rounce, and F. E. Barlow, *J. Phys. E*, 14, No. 2, 229 (1981).
71. I. McWhirter, D. Rees, and A. H. Greenaway, *J. Phys. E*, 15, No. 1, 145 (1982).
72. W. M. Augustyniak, W. L. Brown, and H. P. Lie, *IEEE Trans.*, NS-19, No. 3, 196 (1972).
73. C. W. Gear, Proc. Skytop Conf. on Computer Systems in Experimental Nuclear Physics, USAEC Conf., 670301, USAEC, Washington (1969), p. 552.
74. Advertisement. Surface Sciences Lab. Inc., *Physics Today*, 35, No. 7, 73 (1982); *Phys. Today*, 35, No. 5, 101 (1982).
75. D. G. Smith and K. A. Pounds, *IEEE Trans.*, NS-15, No. 3, 541 (1968).
76. R. Gott, W. Parkes, and K. A. Pounds, *IEEE Trans.*, NS-17, No. 3, 367 (1970).
77. E. Mathieson, K. D. Evans, W. Parkes, and P. F. Christie, *Nucl. Instrum. Methods*, 121, No. 1, 139 (1974).
78. H. A. Van Hoof and M. J. Van der Wiel, *J. Phys. E*, 13, No. 4, 409 (1980).
79. K. Kubierschky, G. K. Austin, D. C. Harrison, and A. G. Roy, *IEEE Trans.*, NS-25, No. 1, 430 (1978).
80. D. Harrison and K. Kubierschky, *IEEE Trans.*, NS-26, No. 1, 411 (1979).
81. E. Kellog, S. Murray, U. Briel, and D. Bardas, *Rev. Sci. Instrum.*, 48, No. 5, 550 (1977).
82. E. M. Kellog, S. S. Murray, and D. Bardas, *IEEE Trans.*, NS-26, No. 1, 403 (1979).
83. G. Knapp, *Rev. Sci. Instrum.*, 49, No. 7, 982 (1978).

84. W. B. Wetherell, in: Applied Optics and Optical Engineering, Vol. 8, Academic Press, New York (1980), p. 171.
85. B. Taylor, Nature, 298, No. 5877, 798 (1982).
86. H. Tananbaum, J. Wash. Ac. Sci., 71, No. 1, 44 (1981).
87. M. C. Weisskopf, J. Wash. Ac. Sci., 71, No. 2, 69 (1981).
88. G. S. Vaiana, J. Wash. Ac. Sci., 71, No. 2, 96 (1981).
89. K. A. Pounds, J. Wash. Ac. Sci., 71, No. 2, 104 (1981).
90. J. Trümper, J. Wash. Ac. Sci., 71, No. 2, 114 (1981).
91. B. G. Taylor, R. D. Andresen, A. Peacock, and R. Zobl, in: X-Ray Astronomy, Proc. XV ESLAB Symp., Reidel, Dordrecht and Boston (1981), p. 479.
92. S. Bower, R. Malina, M. Lampton, et al., Soc. Photo-Opt. Instrum. Eng., 279, 176 (1981).
93. S. Bower and R. F. Malina, J. Wash. Ac. Sci., 71, No. 2, 87 (1981).
94. A. Boksenberg, Nature, 298, No. 5877, 795 (1982).
95. S. P. Worden, Vistas Astron., 20, 301 (1977).
96. G. A. Morton, Appl. Opt., 7, No. 1, 1 (1968).
97. P. A. Eckstrom, J. Appl. Phys., 52, No. 11, 6974 (1981).
98. J. K. Swenson, Bull. Am. Phys. Soc., 27, No. 7, 765 (1982).
99. P. J. Hicks, S. Dariel, B. Wallbank, and J. Comer, J. Phys. E, 13, No. 7, 713 (1980).
100. P. C. Stair, Rev. Sci. Instrum., 51, No. 1, 132 (1980).
101. R. W. Wijnaendts van Resandt, C. de Vreugd, R. L. Champion, and J. Los, Chem. Phys., 29, 151 (1978).
102. T. Odenweller, H. Noll, K. Sapotta, et al., Nucl. Instrum. Methods, 198, No. 1, 263 (1982).
103. V. D. Borisenkov, V. S. Lopatin, V. V. Plotnikov, and I. L. Talov, Elektronnaya Prom., No. 11-12, 17 (1979).
104. M. R. Ainbund, G. S. Vil'dgrube, N. V. Dunaevskaya, et al., Prib. Tekh. Eksp., No. 3, 246 (1982).